Transactions of the 13th International Conference on Structural Mechanics in Reactor Technology (SMiRT 13), Escola de Engenharia - Universidade Federal do Rio Grande do Sul, Porto Alegre, Brazil, August 13-18, 1995

Seismic analysis of rectangular liquid storage structure with submerged objects by a coupled finite element-boundary element method

Koh, H.M., Kim, J., Park, J.-H.
Seoul National University, Dept. of Civil Engineering, Seoul, Korea

ABSTRACT: Seismic analysis of rectangular liquid storage structure is performed by using a coupled boundary element-finite element method. The method models the liquid motion as the irrotation motion of ideal fluid by boundary element method. Coupling with finite element method for the containing structure is performed by using compatibility and equilibrium conditions along the interface of the fluid and structure. Dynamic response characteristics of the fluid-structure interaction system such as sloshing motion, hydrodynamic pressure, displacement, effect of submerged objects are investigated and compared between two- and three-dimensional analysis results.

1. INTRODUCTION

Nuclear spent fuel assemblies are usually stored in a liquid containing reinforced concrete structure of rectangular plane. Under earthquake motions, the structure is known to be subjected to hydrodynamic pressure amplified by the flexibility of liquid containing structure. Free surface sloshing motion due to ground motions is also important for the radioactive protection and thermal effect. The fluid-structure interaction behavior, amplification of hydrodynamic pressure and sloshing motion, in cylindrical type of structure has been extensively investigated and well documented(Housner 1957, Rammerstorfer et al. 1990). For a rectangular liquid containing structure, a two-dimensional coupled boundary element-finite element method has been proposed(Park et al. 1993). However, three-dimensional characteristics of a rectangular container cannot be adequately described by a simple two-dimensional model. This paper presents a general three-dimensional analysis method, and investigates the fluid-structure interaction behavior and the effect of submerged objects inside the container.

The irrotational motion of the inviscid and incompressible ideal fluid is modeled by three-dimensional boundary element method and the motion of structure by finite element method using plate elements. A singularity-free integral formulation is employed for the implementation of boundary element method. Coupling is performed by imposing compatibility and equilibrium conditions along the interface between fluid and structure. The fluid-structure interaction effects are reflected into the coupled equations of motion as added fluid mass matrix and sloshing stiffness matrix. Free surface sloshing motion and hydrodynamic pressure developed in a flexible rectangular container due to ground

motions are computed in time domain and compared with those by two-dimensional analysis. Three-dimensional analysis results show quite new aspects in the dynamic characteristics of the structure and in the pressure distribution pattern along the height and width of the wall. Also investigated are the stability of free-standing objects inside the container and their influence on the overall response of the containing structure.

2. FINITE ELEMENT MODELING OF STRUCTURAL MOTION

The three-dimensional effect should be considered in the modeling of a rectangular liquid storage container since it is composed of plates and slab. Analysis of structural behavior is based on the theory of elasticity and the behavior of rectangular liquid container is modeled by the finite element method using plate elements in three-dimensional analysis(Cook et al. 1989). The three-dimensional analysis of the rectangular liquid container edge is accomplished using transition elements. In two-dimensional analysis the behavior of structure is modeled by plane strain elements.

The finite element equation for the motion of containing structure using plate elements or plane elements can be expressed in the following form:

$$M^s\{\ddot{u}(t)\} + C^s\{\dot{u}(t)\} + K^s\{u(t)\} = f(t) \,, \tag{1}$$

where M^s , C^s and K^s denote mass, damping and stiffness matrices, respectively, $\{u(t)\}$ relative nodal displacement vector, $f(t)$ external nodal force vector.

2. BOUNDARY ELEMENT MODELING OF FLUID MOTION

Three-dimensional motion of inviscid, incompressible, irrotational ideal fluid in a container can be expressed in term of velocity potential. The velocity potential, $\phi(\tilde{x},t)$, satisfies three-dimensional Laplace equation in fluid region .

$$\nabla^2\phi(\tilde{x},t) = 0 \tag{2}$$

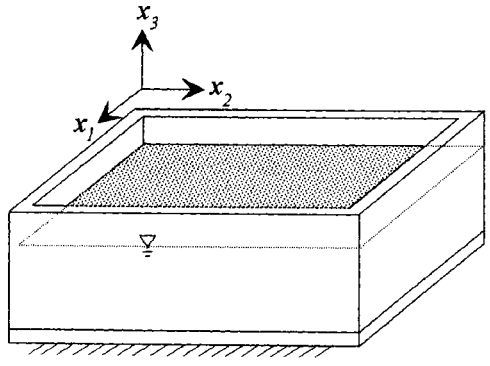

Figure 1 Three-dimensional model and its coordinate system

The governing integral equation of fluid motion is derived from Lagrange-Green Identity.

$$\int_V (G(\tilde{x};\tilde{\xi})\nabla^2\phi(\tilde{x},t) - \phi(\tilde{x},t)\nabla^2 G(\tilde{x};\tilde{\xi}))dV = \int_S G(\tilde{x};\tilde{\xi})\frac{\partial\phi(\tilde{x},t)}{\partial\tilde{n}}ds - \int_S \phi(\tilde{x},t)\frac{\partial G(\tilde{x};\tilde{\xi})}{\partial\tilde{n}}ds \quad (3)$$

In equation (3), $G(\tilde{x};\tilde{\xi})$ is Green's function of Laplace equation,

$$G(\tilde{x};\tilde{\xi}) = \frac{1}{2\pi}\ln(r) \quad : 2\text{-D}$$

$$\frac{1}{4\pi r} \quad : 3\text{-D}$$

were, $\tilde{\xi}$ is the position of source point.
The governing integral equation is rewritten after substituting equation (2) into equation(3).

$$\phi(\tilde{\xi},t) = \int_S \phi(\tilde{x},t)\frac{\partial G}{\partial n}(\tilde{x};\tilde{\xi})ds - \int_S \frac{\partial\phi}{\partial n}(\tilde{x},t)G(\tilde{x};\tilde{\xi})ds \quad (4)$$

A strong singularity occurs in the integral of the first term of equation (4). Equation (4) is thus rearranged into following singularity free from(Rizzo).

$$\phi(\tilde{\xi},t)\int_S \frac{\partial G}{\partial\tilde{n}}(\tilde{x};\tilde{\xi})ds = \int_{S_t}[\phi(\tilde{x},t) - \phi(\tilde{\xi},t)]\frac{\partial G}{\partial\tilde{n}}(\tilde{x};\tilde{\xi})ds + \int_{S_\varepsilon}\phi(\tilde{x},t)\frac{\partial G}{\partial\tilde{n}}(\tilde{x};\tilde{\xi})ds - \int_S \frac{\partial\phi}{\partial\tilde{n}}(\tilde{x},t)G(\tilde{x};\tilde{\xi})ds \quad (5)$$

First two integrals in the right-hand side of equation (5) can be evaluated by usual numerical integration method. The integrand of the last term in equation (5) is weakly singular. The weakly singular integral can be evaluated accurately by using transformation of polar coordinated system.

Applying standard discretization procedure of boundary element method to Equation(5) the following algebraic equations can be obtained

$$[G]\left\{\frac{\partial\phi}{\partial n}\right\} - [T]\{\phi\} = \{0\} \quad (6)$$

where [G] and [T] are coefficient matrices, $\left\{\frac{\partial\phi}{\partial n}\right\}$ and $\{\phi\}$ denote nodal normal velocity vector and nodal potential vector respectively. The singular integrals appearing in the process can be avoided by using an identity related to constant potential field transformation into polar coordinate system.

Linearized dynamic boundary conditions under ground motion derived from Bernoulli equation and kinematic boundary conditions for free surface may be prescribed as(Currie 1974)

$$\frac{\partial\phi}{\partial t}(\tilde{x},t)+g\eta(x_1,x_2,t)=0 \qquad \text{on } S_\eta \tag{7}$$

$$\frac{\partial\phi}{\partial x_3}(\tilde{x},t)=\frac{\partial\eta}{\partial t}(x_1,x_2,t)+\dot{u}_{g3}(t) \quad \text{on } S_\eta \tag{8}$$

Linearized dynamic boundary conditions for the interface between fluid and structure may be prescribed as(Currie 1974)

$$P(\tilde{x},t)=-\rho\frac{\partial\phi}{\partial t}(\tilde{x},t) \qquad \text{on } S_p \tag{9}$$

$$\frac{\partial\phi}{\partial n}(\tilde{x},t)=n\bullet v_p \qquad \text{on } S_p \tag{10}$$

where $\eta(x_1,x_2,t)$ is the vertical displacement of free surface from the stationary level, $P(\tilde{x},t)$ is hydrodynamic pressure in excess of hydrostatic pressure, g is the gravitational acceleration, $\tilde{n}=\tilde{n}(\tilde{x})$ is the exterior normal vector on the boundary, ρ is fluid density. S_η is the boundary of free surface, and S_p is the boundary of the interface between fluid and structure.

Differentiating equation (6) with respect to time and applying boundary conditions, equation (6) can be rewritten as

$$\begin{bmatrix}\mathrm{G}_{pp} & \mathrm{G}_{p\eta}\\ \mathrm{G}_{\eta p} & \mathrm{G}_{\eta\eta}\end{bmatrix}\left\{\frac{\partial}{\partial t}\left(\frac{\partial\phi}{\partial n}\right)\right\}+\begin{bmatrix}\mathrm{T}_{pp} & \mathrm{T}_{p\eta}\\ \mathrm{T}_{\eta p} & \mathrm{T}_{\eta\eta}\end{bmatrix}\left\{\frac{\partial\phi}{\partial t}\right\}=\{0\}$$

$$\begin{bmatrix}\overline{\mathrm{G}}_{pp} & \mathrm{G}_{p\eta}\\ \overline{\mathrm{G}}_{\eta p} & \mathrm{G}_{\eta\eta}\end{bmatrix}\begin{Bmatrix}\dot{\mathrm{v}}_p\\ \ddot{\eta}+\{1\}\ddot{u}_{g3}\end{Bmatrix}+\begin{bmatrix}\overline{\mathrm{T}}_{pp} & \overline{\mathrm{T}}_{p\eta}\\ \overline{\mathrm{T}}_{\eta p} & \overline{\mathrm{T}}_{\eta\eta}\end{bmatrix}\begin{Bmatrix}\mathrm{P}\\ \eta\end{Bmatrix}=\{0\} \tag{11}$$

where, $\overline{G}_{pp} = G_{pp} \bullet \tilde{n}$, $\overline{G}_{\eta p} = G_{\eta p} \bullet \tilde{n}$,

$\overline{T}_{pp} = T_{pp} / \rho$, $\overline{T}_{\eta p} = T_{\eta p} / \rho$,

$\overline{T}_{p\eta} = gT_{p\eta}$, $\overline{T}_{\eta\eta} = gT_{\eta\eta}$

In equation(11) $\dot{v}_p$, P and η are nodal acceleration, nodal pressure on the interface boundary, and nodal displacement on the free surface. The upper partition of equation (11) is solved for pressure and then the equations of hydrodynamic pressure acting on the wall can be written as

$$P = P_1\{\dot{v}_p\} + P_2\{\ddot{\eta}\} + P_3\{\eta\} + P_2\{1\}\ddot{u}_g \tag{12}$$

where, $P_1 = \overline{T}_{pp}^{-1}\overline{G}_{pp}$, $P_2 = \overline{T}_{pp}^{-1}\overline{G}_{p\eta}$, $P_3 = \overline{T}_{pp}^{-1}\overline{T}_{p\eta}$

Thus, the equations of fluid motion can be written as

$$M_{\eta p}\{\dot{v}_p\} + M_{\eta\eta}\{\ddot{\eta}\} + K_{\eta\eta}\{\eta\} + M_{\eta\eta}\{1\}\ddot{u}_{g3} = \{0\} \tag{13}$$

where, $M_{\eta p} = \overline{G}_{\eta p} - \overline{T}_{\eta p}\overline{T}_{pp}^{-1}\overline{G}_{pp}$,

$M_{\eta\eta} = G_{\eta\eta} - \overline{T}_{\eta p}\overline{T}_{pp}^{-1}G_{p\eta}$,

$K_{\eta\eta} = \overline{T}_{\eta\eta} - \overline{T}_{\eta p}\overline{T}_{pp}^{-1}\overline{T}_{p\eta}$

In a rigid container, equation (13) is defined in terms of only $\eta, \ddot{\eta}$ since acceleration $\dot{v}_p$ is identical to the ground acceleration, $\ddot{u}_g$.

COUPLING PROCEDURE

The finite element equation of structural motion for the container subjected to ground motions can be written as

$$M^s\{\ddot{u}(t)\} + K^s\{u(t)\} = -M^s[r^s]\{\ddot{u}_g(t)\} + f(t) \tag{14}$$

where M^s and K^s represent mass and stiffness matrix, respectively. $u(t)$ is relative nodal displacement , $\ddot{u}_g(t)$ is ground acceleration, r^s is earthquake influence coefficient matrix, $f(t)$ is external nodal force. Since the discretized equation of fluid motion is expressed in

terms of displacement and acceleration, it can be coupled directly with finite element equation of the structure. To facilitate coupling, absolute acceleration $\dot{v}_p$ in equation (13) is replaced by relative acceleration, $\ddot{u}_c$, and the ground acceleration, $\ddot{u}_g$.

$$M_{\eta p}\{\ddot{u}_c\} + M_{\eta\eta}\{\ddot{\eta}\} + K_{\eta\eta}\{\eta\} = -M_{\eta p}\{\ddot{u}_g\} - M_{\eta\eta}\{1\}\ddot{u}_{g3} \tag{15}$$

Along the interface between the walls and fluid, compatibility and equilibrium equations should be satisfied. Fluid particle acceleration normal to the interface boundary is set to equal to the acceleration of the structure boundary in the same direction under the assumption of small displacement. In order to impose equilibrium condition at the coupled nodes, traction distribution is converted into equivalent nodal forces. Equivalent nodal force vector can be related to nodal pressure vector by using distribution matrix L as

$$f = -LP = -M_{pp}\{\ddot{u}_c\} - M_{p\eta}\{\ddot{\eta}\} - K_{p\eta}\{\eta\} - M_{pp}\{\ddot{u}_g\} - M_{p\eta}\{1\}\ddot{u}_{g3} \tag{16}$$

where, $M_{pp} = -L\bar{T}_{pp}^{-1}\bar{G}_{pp}$, $M_{p\eta} = -L\bar{T}_{pp}^{-1}\bar{G}_{p\eta}$, $K_{p\eta} = -L\bar{T}_{pp}^{-1}\bar{T}_{p\eta}$

Replacement of external pressure force by an equivalent nodal force and addition of equation (15) yield dynamic equation of coupled system including fluid free surface motion.

$$\begin{bmatrix} M^s_{oo} & M^s_{op} & 0 \\ M^s_{po} & M^s_{pp}+M_{pp} & M_{p\eta} \\ 0 & M_{\eta p} & M_{\eta\eta} \end{bmatrix}\begin{Bmatrix}\ddot{u}_o\\ \ddot{u}_p\\ \ddot{\eta}\end{Bmatrix} + \begin{bmatrix} K^s_{oo} & K^s_{op} & 0 \\ K^s_{po} & K^s_{cc} & K_{p\eta} \\ 0 & 0 & K_{\eta\eta} \end{bmatrix}\begin{Bmatrix}u_o\\ u_p\\ \eta\end{Bmatrix} = -\begin{bmatrix} M^s_{oo} & M^s_{op} & 0 \\ M^s_{po} & M^s_{pp}+M_{pp} & M_{p\eta} \\ 0 & M_{\eta p} & M_{\eta\eta} \end{bmatrix}[r]\{\ddot{u}_g\} \tag{17}$$

where u_o, $\ddot{u}_o$ are nodal displacement and acceleration for the nodes of structure which are not in contact with fluid, u_p, $\ddot{u}_p$ are those in contact with fluid and r is earthquake influence coefficient matrix. The effect of fluid-structure interaction is reflected by added mass matrix of internal fluid and sloshing stiffness matrix. The coefficient matrices in the left-hand side of equation (17) depends on the geometric characteristics and material properties of coupled system. For a case in which convective term due to sloshing motion is neglected, the equation of the coupled system is

$$\begin{bmatrix} M^s_{oo} & M^s_{op} \\ M^s_{po} & M^s_{pp}+M_{pp} \end{bmatrix}\begin{Bmatrix}\ddot{u}_o\\ \ddot{u}_p\end{Bmatrix} + \begin{bmatrix} K^s_{oo} & K^s_{op} \\ K^s_{po} & K^s_{cc} \end{bmatrix}\begin{Bmatrix}u_o\\ u_p\end{Bmatrix} = -\begin{bmatrix} M^s_{oo} & M^s_{op} & 0 \\ M^s_{po} & M^s_{pp}+M_{pp} & M_{p\eta} \end{bmatrix}[r^i]\{\ddot{u}_g\} \tag{18}$$

where, r^i is earthquake influence coefficient matrix including impulsive term only.

NUMERICAL EXAMPLES

Dynamic responses of the fluid-structure system described in Figure 2 are analyzed by two- and three-dimensional coupled boundary element-finite element methods. For the present paper, analysis results for the excitation in the x_1 direction only are presented. The N-S component of the ground acceleration recorded at El Centro in the 1940 Imperial Valley Earthquake is used as input motion with peak ground acceleration adjusted to 0.2g.

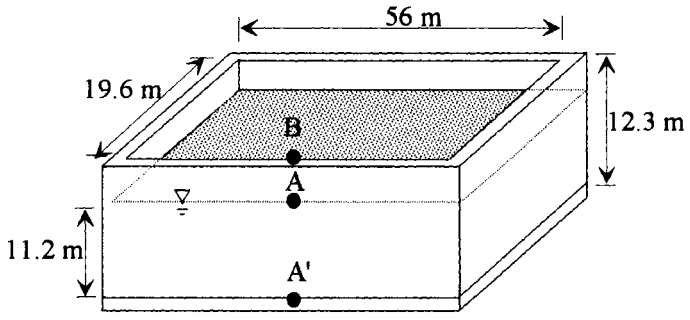

$E = 21.00 \times 10^9\ N/m^2$

$\rho = 2400\ Kg/m^3$

$\nu = 0.17$

(a) Three dimensional model

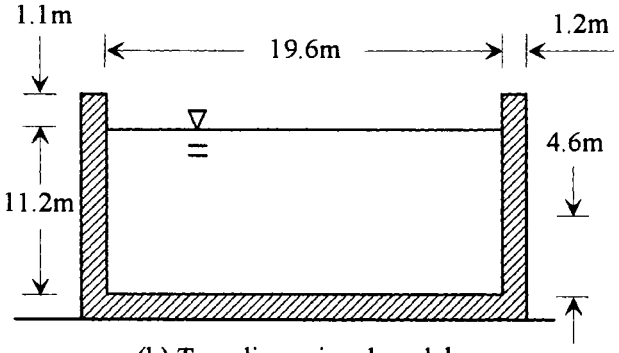

(b) Two dimensional model

Figure 2 Dimensions and material properties of rectangular container model

Given in Figure 3 are time histories of the free surface sloshing motion at observation point A in Figure 2, which shows that the wall flexibility introduces higher modes of sloshing motion. It is recognized that the overall trends are quite similar between two- and three-dimensional analysis with minor difference in their detailed shapes. Displacement time histories at the top of the structure (observation point B in Figure 2) are provided in Figure 4. The natural frequency of three-dimensional model is shown to

be slightly higher than that of two-dimensional model because of increased constraint effect in three-dimensional model. But there are not any notable differences in general trend and magnitude between the two-dimensional and the three-dimensional analysis results for the displacement at the top of wall. However the base shear is amplified due to the three-dimensional effect of fluid and structure(Figure 5). The magnitude and distribution pattern of the developed hydrodynamic pressure, amplified by the wall flexibility, are significantly different between the two-dimensional and the three-dimensional analysis. Figure 6 and 7 show hydrodynamic pressure distribution at the instance when the base shear reaches its peak value. In Figure 6, pressure distribution curves along the height of the wall(AA' in Figure 2) are compared between the two analyses. It shows that amplification of the pressure in three-dimensional model is much more pronounced than that in two-dimensional model. But this kind of amplification is developed only around the middle of the wall in the x_2 direction as can be seen in the spatial distribution pattern of the pressure over the wall surface(Figure 7).

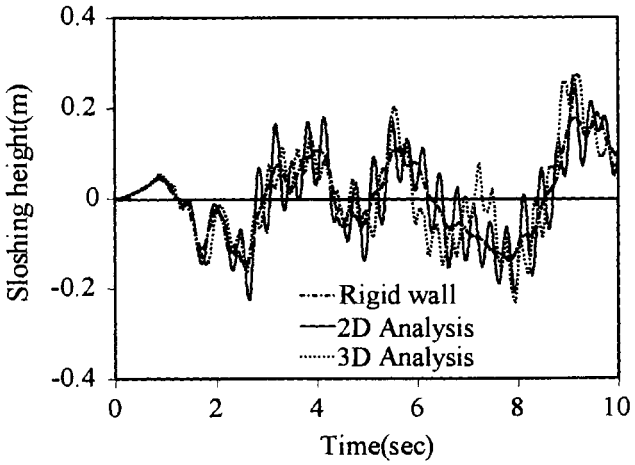

Figure 3 Histories of free surface sloshing at the intersection point

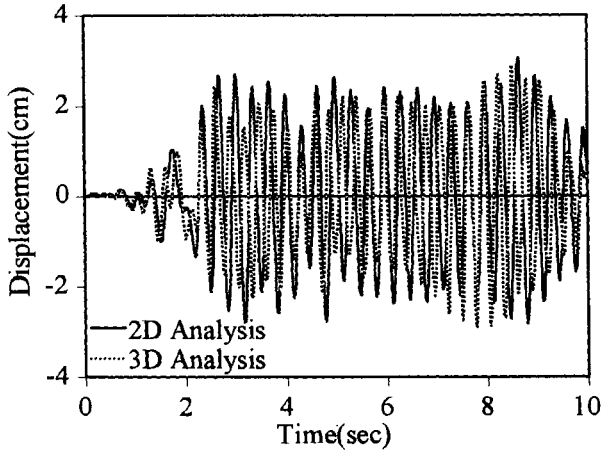

Figure 4 Histories of displacement at the top of the wall

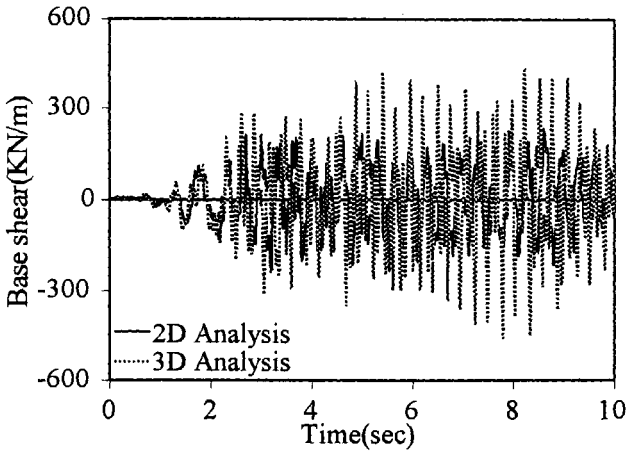

Figure 5 Histories of base shear acting on the wall

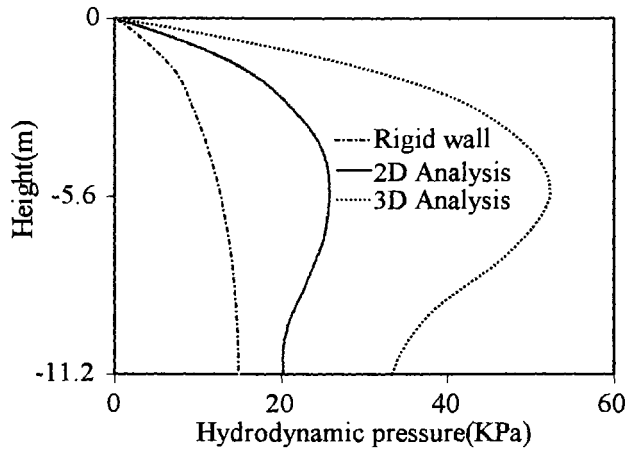

Figure 6 Hydrodynamic pressure distribution along the wall

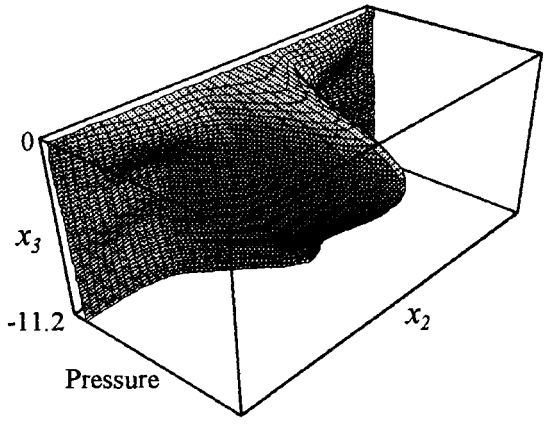

Figure 7 Spacial distribution of hydrodynamic pressure

It is of interest to investigate the effect of submerged objects on the response of fluid-structure system under the ground excitation. The complete study of this problem may require extensive three-dimensional analysis, however, for the present paper, analysis results by two-dimensional model are mostly presented and compared with selective analysis results by three-dimensional model. Two-dimensional analysis model is presented in Figure 8. The model shown in Figure 8 would represent a situation in which many submerged objects are arranged densely in three rows running in the x_2 direction. The submerged object under consideration is quite heavy and stiff, thus they are assumed to be rigid and fixed to the base slab for the analysis purpose. The submerged object have square cross section(0.8m × 0.8m). The profiles of fluid surface motion obtained by two-dimensional analysis are compared in Figure 9. Free surface sloshing motion is shown to be very sensitive to the presence of submerged objects although the maximum sloshing heights are identical. Time histories of acceleration at the top of the structure(point B) are given in Figure 10, and pressure distribution along the height of the wall in Figure 11.

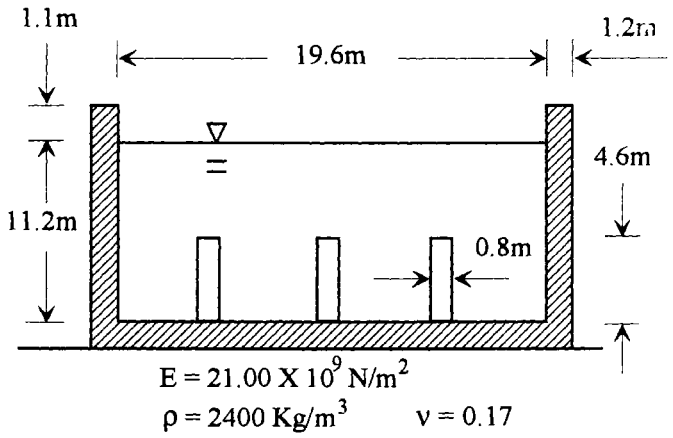

Figure 8 Dimensions and material properties of rectangular container with submerged objects

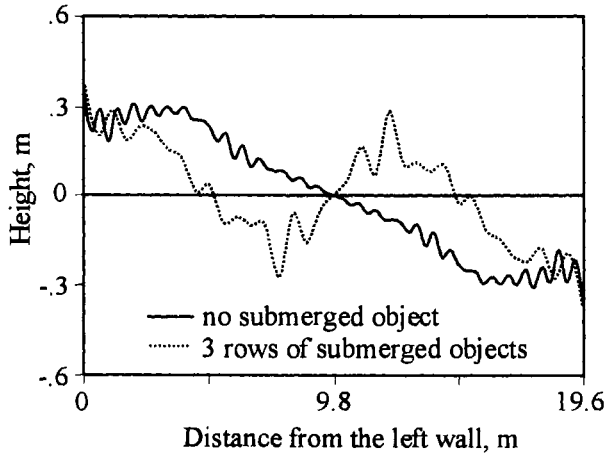

Figure 9 Profiles of fluid surface

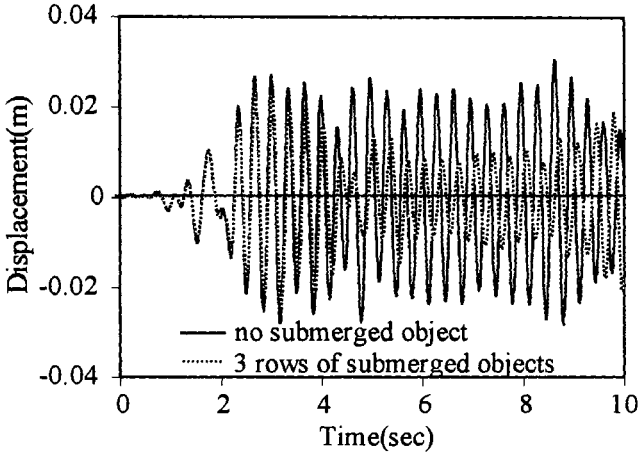

Figure 10 Histories of displacement at the top of the wall

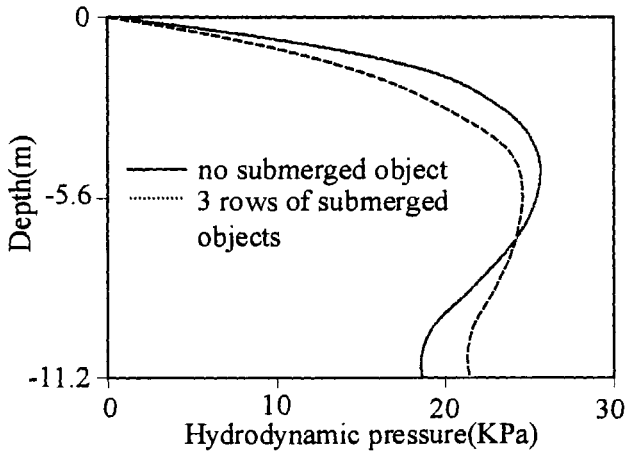

Figure 11 Hydrodynamic pressure distribution along the height of wall

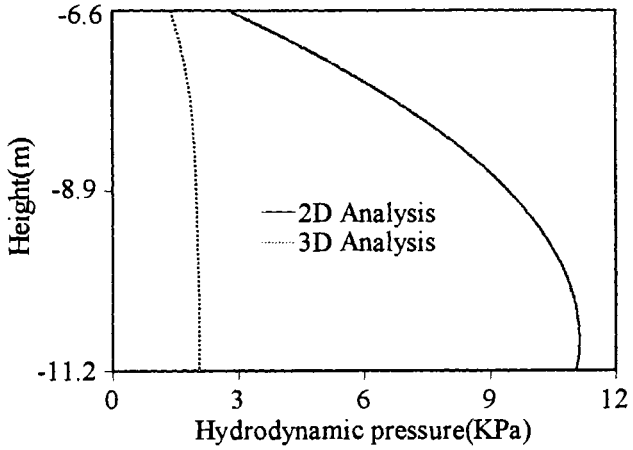

Figure 12 Hydrodynamic pressure distribution along the submerged object

Slight change in the distribution pattern of the hydrodynamic pressure indicates the reduction of fluid-structure interaction effect. Preliminary study by a three-dimensional model shows that free surface sloshing and pressure distribution along the height of the wall are not greatly affected due to the presence of submerged object. However the magnitude and distribution pattern of hydrodynamic pressure acting along the height of submerged object are significantly different between two-dimensional and three-dimensional analyses(Figure 12). The pressure distribution around the object is calculated at the moment when the base shear reaches its peak value for a case of only one submerged object at the center of slab. From the pressure distribution, the force acting on the object in two-dimensional analysis is overestimated and, therefore, three-dimensional analysis may be required for the stability study of submerged objects.

CONCLUSIONS

Dynamic response characteristics of rectangular liquid container, usually used for the wet storage of nuclear spent fuel assemblies, have been investigated by using a coupled boundary element-finite element method. While the magnitude and distribution pattern of hydrodynamic pressure acting on the wall are found to be significantly different between two- and three-dimensional analysis results, free surface sloshing motion and displacement of the wall show quite similar behaviors between the two analyses. The base shear is predicted to be much more amplified by three-dimensional analysis. Natural frequency of the coupled system is also predicted to be higher in three-dimensional model than in two-dimensional model. Preliminary study on the effect of submerged objects shows that although the profile of fluid surface is quite sensitive to the presence of submerged objects there is not any change in the maximum sloshing height. Hydrodynamic pressure acting on the height of submerged object, however, predicted by two-dimensional analysis is significantly overestimated. It is therefore recommended that three-dimensional analysis be used for the investigation of hydrodynamic pressure distribution.

REFERENCES

Cook, Robert D., David S. Malkus and Michael E. Plesha 1989. *Concepts and Application of Finite Element Method.* John Wiley & Sons Inc.

Currie, I. G. 1974. *Fundamental Mechanics of Fluids.* McGraw-Hill Inc.

Housner, George W. 1957. Dynamics Pressure On Accelerated Fluid Container. *Bulletin of the Seismological Society of America*, vol. 47: 15-35.

Park, J.-H., H.M. Koh, J. Kim 1993. Dynamic Analysis of Liquid Storage Rectangular Container by a Coupled Boundary Element-Finite Element Method. *Proc. of EASEC-4:* 1815-1820. Seoul, Korea.

Rammerstorfer, Franz G., Kunt Scharf and Franz D. Fisher 1990. Storage tanks under earthquake loading. *Applied Mechanics Reviews*, ASME, Vol. 43: 261-282.

Rizzo, F. J., D. J. Shippy and M. Rezayat A Boundary Integral Equation Method For Radiation And Scattering of Elastic Waves In Three Dimensions. *Internaitonal Journal For Numerical Methods In Engineering*, Vol. 21: 115-129.